ORIGINAL RESEARCH

Short-term Medication Effects on Brain Functional Activity and Network Architecture in First-Episode psychosis: a longitudinal fMRI study

Yajuan Zhang[1] · Qiong Xiang[2] · Chu-Chung Huang[3] · Jiajia Zhao[1] · Yuchen Liu[1] · Ching-Po Lin[1,4] · Dengtang Liu[2,5,6] · Chun-Yi Zac Lo[1]

Abstract

The effect of antipsychotic medications is critical for the long-term outcome of symptoms and functions during first-episode psychosis (FEP). However, how brain functions respond to the antipsychotic treatment in the early stage of psychosis and its underlying neural mechanisms remain unclear. In this study, we explored the cross-sectional and longitudinal changes of regional homogeneity (ReHo), whole-brain functional connectivity, and network topological properties via resting-state functional magnetic resonance images. Thirty-two drug-naïve FEP patients and 30 matched healthy volunteers (HV) were included, where 23 patients were re-visited with effective responses after two months of antipsychotic treatment. Compared to HV, drug-naive patients demonstrated significantly different patterns of functional connectivity involving the right thalamus. These functional alterations mainly involved decreased ReHo, increased nodal efficiency in the right thalamus, and increased thalamic-sensorimotor-frontoparietal connectivity. In the follow-up analysis, patients after treatment showed reduced ReHo and nodal clustering in visual networks, as well as disturbances of visual-somatomotor and hippocampus-superior frontal gyrus connectivity. The longitudinal changes of ReHo in the visual cortex were associated with an improvement in general psychotic symptoms. This study provides new evidence regarding alterations in brain function linked to schizophrenia onset and affected by antipsychotic medications. Moreover, our results demonstrated that the functional alterations at baseline were not fully modulated by antipsychotic medications, suggesting that antipsychotic medications may reduce psychotic symptoms but limit the effects in regions involved in disease pathophysiology.

Keywords Longitudinal study · Resting-state fMRI · Antipsychotic treatment · Brain activity · Graph theoretical analysis

✉ Dengtang Liu
liudengtang@smhc.org.cn

✉ Chun-Yi Zac Lo
zaclocy@gmail.com

[1] Institute of Science and Technology for Brain-Inspired Intelligence (ISTBI), Fudan University, 220 Handan Road, 200433 Shanghai, PR China

[2] First-episode Schizophrenia and Early Psychosis Program, Division of Psychotic Disorders, Shanghai Mental Health Center, Shanghai Jiao Tong University School of Medicine, 600 Wanping South Road, 200030 Shanghai, China

[3] Institute of Cognitive Neuroscience, School of Psychology and Cognitive Science, East China Normal University, Shanghai, China

[4] Institute of Neuroscience, National Yang-Ming University, 11221 Taipei, Taiwan

[5] Shanghai Key Laboratory of Psychotic Disorders, Shanghai Mental Health Center, Shanghai Jiao Tong University School of Medicine, 200030 Shanghai, China

[6] Institute of Mental Health, Fudan University, 200030 Shanghai, China

Introduction

Schizophrenia is a neurodevelopmental disorder characterized by a persistent or recurrent process (Dixon et al., 1999). First-episode psychosis (FEP) is characterized by the initial experience of psychosis. Studies have shown that about 3 out of 100 people will experience their first episode of psychosis at some point in their lives and has a 70% chance of developing into a chronic condition (Elhamaoui et al., 2003; McGrath et al., 2008). Early treatment provides a foundation for recovery and whole life, even if some patients continue to experience symptoms (Tarcijonas & Sarpal, 2019). Therefore, monitoring cerebral function in patients with FEP before and after treatment is helpful in understanding the intrinsic functional alterations of the brain underlying the onset of psychosis, as well as the mechanisms of therapeutic benefits of antipsychotic medication.

Advanced resting-state functional magnetic resonance imaging (rs-fMRI) can reflect brain activation via blood oxygenation level-dependent signals. Studies have shown that patients with FEP have abnormal brain activity and neural circuitry function. By employing amplitude of low-frequency fluctuations (ALFF), fractional ALFF (fALFF), and regional homogeneity (ReHo), the abnormal regional/local spontaneous activity in various brain regions has been found in drug-naïve FEP patients such as the prefrontal cortex, inferior parietal lobule, caudate and putamen (He et al., 2013; Hu et al., 2016; Huang et al., 2010; Li et al., 2016b). These regional abnormalities have also been found to be related to altered functional connectivity in FEP (Li et al., 2016a; Lui et al., 2010), indicating that the regional changes can reorganize brain networks (i.e., between regional dysfunctions). Considering the brain as a complex network with a macroscopic organization, topological metrics are commonly used to characterize the organization of the relationships between elements (i.e., brain regions) in the system-level aspect (Bullmore & Sporns, 2009). A randomization structure has been revealed in chronic schizophrenia, as well as in drug-naïve FEP patients, indicating a higher speed of information transfer and decreased local interactions between brain regions (Lo et al., 2015; van den Heuvel et al., 2013; Wang et al., 2019). Furthermore, changes in FC or functional network topology have also been found in high-risk healthy subjects (Del Fabro et al., 2021; Lo et al., 2015).

In longitudinal fMRI studies, regional activation and neural circuitry patterns have been significantly altered after short-term antipsychotic treatment in FEP (Li et al., 2016b; Lui et al., 2010; Sarpal et al., 2015). Notably, the resting-state functional connectivity (FC) in FEP was increased after antipsychotic treatment and was found to be correlated with improved symptoms (Nina et al., 2016; Sarpal et al., 2015). Other similar studies also found that antipsychotic medications could affect FC, but these alterations do not have a correlation with relief of clinical psychotic symptoms (Guo et al., 2018; Kraguljac et al., 2016; Wang et al., 2017). In addition, aberrant integration and segregation patterns of brain networks have been found to be modulated by antipsychotic medications (Hadley et al., 2016; Wang et al., 2019), however, one study found no evidence of abnormal topology in FEP participants compared to healthy controls and no evidence of change after 12-month medication treatment (Ganella et al., 2018). Furthermore, FEP patients who responded to treatment exhibit specific network characteristics compared to nonresponding FEP patients (Crossley et al., 2017). Given the evidence of medication-related FC and network changes in psychosis, these findings could serve as possible biomarkers for treatment assessment. However, the lack of a local to global assessment to evaluate the brain function deficit of FEP.

In this study, we performed a systematic analysis to examine differences in spontaneous neural activity and topological organizations between FEP patients and controls at baseline, followed by a longitudinal study to examine the effects of antipsychotic treatment on functional changes between patients at baseline and follow-up. We hypothesize that (i) abnormal brain function measurements would be revealed in the early stages of schizophrenia; (ii) short-term antipsychotic medications would modulate neural activity and network topology architecture, and abnormal brain functional measurements would be associated with clinical improvement.

Materials and methods

Participants

A total of 34 drug-naïve first-episode psychosis patients (FEP-dn) were recruited from outpatient at the Shanghai Mental Health Center. All patients met the criteria of the *Diagnostic and Statistical Manual of Mental Disorders-IV* for schizophrenia or schizophreniform disorder (Association, 1994), and a research psychiatrist confirmed the diagnosis. All of them did not have any form of antipsychotic treatment before the initial scan. Patients diagnosed with schizophreniform disorder at the time of study enrollment were subsequently diagnosed with schizophrenia six months later. The exclusion criteria for patients included any history of significant head injury, mental retardation, substance abuse, antipsychotic treatment, comorbid mental health diagnoses, significant medical conditions, such as severe cardiovascular, hepatic, and renal diseases and pregnancy or breastfeeding, the presence of standard MRI

Table 1 Demographic information for drug-naive first-episode psychosis and healthy volunteers

Characteristics	Drug-naïve First Episode Psychosis (FEP-dn N = 32)	Healthy Volunteers (HV: N = 30)	*P*-value
Age(years)	26.8 ± 6.1	27.1 ± 4.3	0.82[a]
Male/Female	15/17	15/15	0.8[b]
Education(years)	12.9 ± 3.2	14.3 ± 2.5	0.06[a]

Data were presented as mean ± SD; FEP-dn: drug-naïve first episode psychosis patients; HV: healthy volunteers;

[a]*P*: two-sample t-test

[b]*P*: Pearson chi-squares

contraindications (e.g., metal implants, claustrophobia, current pregnancy, or breastfeeding). Thirty healthy volunteers (HV) were recruited from the local community through advertising. These healthy people did not have mental disorders, neurological diseases, a positive family history of mental illness, and no known first-degree relative with psychotic disease. The study was approved by Shanghai Mental Health Center, Shanghai, China. All participants gave their informed consent in writing.

Quality control was performed on the imaging data. Two participants were excluded due to excessive head motion (exceeding 2 mm of translational movement, 2° of rotational movement). Then, we calculate an instantaneous head motion termed framewise displacement (FD) as a covariate in the subsequent statistical analysis. There was no significant group difference in mean framewise displacement (FD) between the remaining baseline patients and HV (FEP: 0.09 ± 0.03; HV: 0.10 ± 0.04; P = 0.42, two-sample t-test). Finally, as shown in Table 1, a total of 62 participants were included in this study, including 32 baseline FEP patients and 30 HV (FEP-dn: n = 32, mean age = 26.8 ± 6.1 years; HV: n = 30, mean age = 27.1 ± 4.3 years). Among the patients, twenty-three of the baseline patients completed a second MRI scanning at two months (FEP-2 m: n = 23).

Medication and clinical assessment

All FEP patients were treated with second-generation antipsychotics (SGA) for two months. Choices and doses of the drugs were determined on the basis of clinical judgment. More information on the medication and dose for each patient can be found in Table S1. The severity of symptoms in FEP patients was assessed using 30 items of the Positive and Negative Syndrome Scale (PANSS), including the positive scale (PANSS-P, 7 items), the negative scale (PANSS-N, 7 items), and the general psychopathology scale (PANSS-G, 16 items) (Kay et al., 1987). Each item was rated from 1 to 7, ranging from no symptoms to severe symptoms.

MRI data acquisition

This study was carried out on a 3.0T Siemens Verio MR Scanner (Siemens AG, Erlangen, Germany) with a 32-channel head coil at the Shanghai Mental Health Center. During the magnetic resonance scanning, all subjects lay supine with inflatable pillows for minimal head motion. Anatomical T1-weighted images were acquired using a magnetic preparation fast gradient echo (MPRAGE) sequence with echo time = 3.65 ms, repetition time = 2530 ms, field of view = 256 * 256 mm, slice thickness = 1.0 mm and slice number = 224. The fMRI data were acquired using an echo-planar scanning sequence in which the participants were instructed to remain awake with their eyes closed and avoid systematic thinking. The fMRI parameters were as follows: number of axial slices = 30, slice thickness = 4.0 mm with a 1 mm gap between slices, repetition time = 2000 ms, echo time = 30 ms, field of view = 220 * 220 mm, 64 * 64 matrix, flip angle = 90°, total volumes measurement = 180.

fMRI preprocessing

The preprocessing of the rs-fMRI data was implemented with Analysis of Functional NeuroImages (AFNI, https://afni.nimh.nih.gov) and the FMRIB software library (FSL v5.02, https://fsl.fmrib.ox.ac.uk/fsl/fslwiki). The initial ten volumes were discarded for each individual, and the preprocessing included the following steps. Slice-timing and motion correction to the first volume with rigid-body alignment were performed. Wavelet despiking was applied to aligned images to remove signal transients related to small-amplitude (< 1 mm) head movements (Patel et al., 2014). Multiple regression was used to remove the contributions of motion parameters and their first derivatives, the global average white matter, and cerebrospinal fluid signals from the fMRI time series data. A temporal band-pass filter (0.01–0.1 Hz) was applied to reduce the effects of low- and high-frequency physiological noise. The fMRI data were spatially normalized to the standard space of $3 \times 3 \times 3$ mm^3 of the Montreal Neurological Institute (MNI) by first aligning the functional images with the structural images of the subject's T1 using a boundary-based registration (Greve & Fischl, 2009) and then transforming them into standard space (FSL flirt and fnirt). Finally, the images were spatially smoothed by a Gaussian kernel with full width at a half maximum of 6 mm (spatial smoothing was not performed before the ReHo calculation).

Functional activity estimation

ReHo estimates functional similarities in brain activity among neighboring voxels within a short-range (Zang et al., 2004). Individual ReHo maps were determined on a voxel-by-voxel basis by calculating Kendall's coefficient concordance of the time series of a given voxel with those of its nearest 26 neighbors without spatial smoothing. For standardization purposes, the ReHo value of each voxel was divided by the whole-brain mean ReHo value.

Brain functional network construction

The gray matter of the cerebrum was segmented into 94 cortical and subcortical regions (47 in each hemisphere) using the automated anatomical labeling 2 (AAL2) atlas (Rolls et al., 2015). Each region acted as the node of the functional brain network. We assign AAL2 regions to Yeo's seven functional networks according to the most overlapping ratio (the percentage of voxels of a specific region with each network) (Yeo et al., 2011). The subcortical areas were added as an additional network. Pearson correlation coefficients were calculated between the regional mean time series of all possible pairs of 94 brain regions and the z-transformed correlation coefficients to generate 94×94 whole-brain FC matrices for each subject. The results of the FC analysis were visualized using Circos software (http://circos.ca/software/download/).

Brain functional network analysis

Global topology of functional networks: Absolute FC matrices were used to construct undirected binary graphs. Binary network metrics were calculated for each individual with connection density in the range of 1–100% in increments of 1%. Global topological parameters for each connection density of brain networks were calculated, including the small-world parameters [clustering coefficient (C_p), characteristic path length (L_p), normalized clustering coefficient (γ), normalized characteristic path length (λ), and scalar small-worldness (σ)], and network efficiency [global efficiency (E_g) and local efficiency (E_{loc})]. To examine the small-world properties, we generated 100 matched random networks with the same number of nodes, edges, and degree distribution as real networks. We then defined the normalized clustering coefficient (γ), $\gamma = C_p^{real}/C_p^{rand}$, normalized characteristic path length (λ), $\lambda = L_p^{real}/L_p^{rand}$, where L_p^{rand} and C_p^{rand} are the mean clustering coefficient and the mean shortest path length of 100 matched random networks. If a network meets the conditions that $\gamma > 1$ and

$\lambda \approx 1$ or $\delta = \gamma/\lambda > 1.1$, the network has small-world properties (Watts & Strogatz, 1998). The area under the curve for each network metric was calculated for statistical comparisons between patients and control groups, providing a summarized scalar for topological properties.

Network module structure: The module is defined as a set of relatively sparse connections with the nodes in the external module, while the nodes in the internal module are highly interconnected (Girvan & Newman, 2002). To detect functional brain modules for each group, we calculated a group-level FC matrix by averaging all individual-level FC matrices and applied a modified greedy optimization algorithm to detect the modular structure of each group (Clauset et al., 2004). When the maximum value of network modularity meets the conditions that $Q > 0.3$ indicates that the network has a modular structure.

Degree distribution: The degree distribution of a small-world functional network was used to summarize nodal degree over the whole brain (Achard et al., 2006). Network degree distribution was estimated under the small-world regime corresponding to a connection density of 10–40% (the minimum density 10% maintains the network integrity, minimizing the number of disconnected nodes, and the maximum density 40% guarantees the small-world network properties) (Watts & Strogatz, 1998). Based on published literature, the probability distribution of degree over all nodes in the network under a small-world regime was best fit by the nonlinear fitting function using an exponentially truncated power law: $P(k) = a*k^{alpha-1}*e^{-k/k_c}$, where k denotes degree, the parameters of this distribution are the constant-coefficient, a, the power-law exponent, alpha, and the exponential cutoff, k_c (Achard et al., 2006; Lo et al., 2015). In the group comparison analysis, we tested whether its parameters, *a, alpha*, and k_c, were altered in the cross-sectional and longitudinal studies.

Nodal topology: In the small-world regime corresponding to 10–40% connection density, nodal clustering (C_{p_node}) and nodal efficiency (E_{g_node}) were also estimated for each node. C_{p_node} is defined as the ratio of the existing connections to all possible links in the nearest neighbors of the node. E_{g_node} reveals the information dissemination ability between a node and the rest of the nodes in the network. Graph theoretical analysis was performed using the GRETNA toolbox (Wang et al., 2015). Network analysis results were visualized using BrainNet Viewer software (http://www.nitrc.org/projects/bnv/).

Correlation analysis

Once between-group differences were determined in any fMRI measurements, a series of partial correlation analyses were performed to examine the associations of these fMRI measurements with medication dosage and PANSS scores (i.e., PANSS-P, PANSS-N, PANSS-G, and total scores), with age, sex, education, and mean FD being regressed ($P < 0.05$, uncorrected). First, to determine whether the altered ReHo/network measures could be predicted by FEP-related clinical symptoms at baseline, a correlation analysis was performed between fMRI measurements and FEP-dn PANSS scores. Second, to compare the dose of medications and changes in the PANSS ratings with longitudinal changes in functional measurements in the FEP group, the relationship between the changes of ReHo and network parameters (follow-up minus baseline) and the improvement in the PANSS scores (baseline PANSS-G scores minus follow-up PANSS-G scores) was evaluated.

Statistical analysis

Differences in demographic characteristics between HV and baseline FEP patients were tested using a two-sample t-test (age and education) and Chi-square tests (sex). PANSS scores in the FEP before and after treatment were compared using a paired t-test. The tests were two-tailed and the significant level was $P < 0.05$. Comparisons between FEP-dn and HC were performed using two-sample t-tests, with age, sex, education and mean FD as covariates, and longitudinal comparisons between the pre-treatment and post-treatment patients with FEP were tested using a paired t-test, with the mean FD as a covariate. The different multiple comparison strategies for the t-tests were applied. i) For ReHo analysis, the significance threshold was set at $P < 0.001$ in the voxel level, followed by the Gaussian random field (GRF) correction at the cluster level of $P < 0.05$. ii) For the network topological parameters, the statistical significance level for global parameters (γ, λ, σ, C_p, L_p, E_g, and E_{loc}) were set $P < 0.05/7 = 0.007$ (Bonferroni correction), and the statistical significance level for regional properties (C_{p_node} and E_{g_node}) were set $P < 0.05$ (FDR correction). iii) For whole-brain FC, the framework of the network-based statistical approach (NBS) was applied to detect differences in FC between HV and FEP-dn. In brief, a primary cluster-defining threshold ($P < 0.001$) was first used to identify all the suprathreshold connected subnetworks, and their sizes (the number of links) were then determined. Then, an empirical null distribution of maximal component sizes under the null hypothesis of random group membership (5000 permutations) was used to calculate the corrected p-value < 0.05 for each component. As the paired sample is not applicable to

Table 2 Clinical symptoms in drug-naive first-episode psychosis before and after 2 months of treatment with antipsychotic medication and dosages

	First Episode Psychosis (FEP)		P-value
	FEP-dnp (N=23)	FEP-2 m (N=23)	
PANSS scores			
PANSS-P	19.8 ± 5.6	11.2 ± 3.6	8.44E-07[c]
PANSS-N	17.7 ± 6.7	12.4 ± 4.9	0.0023[c]
PANSS-G	38.1 ± 10.3	25.0 ± 6.7	1.43E-05[c]
Total	75.6 ± 19.6	48.6 ± 14.1	5.18E-06[c]
SGAs dose[d] (CPZE, mg)		335.7 ± 145.9 (N=22)	

Data were presented as mean $\pm$ SD

FEP-2 m: FEP patients with two-month antipsychotics treated; FEP-dnp: the drug-naïve FEP patients paired with FEP-2 m. SGAs: second-generation antipsychotics

[c] P: Paired t-test

[d] The daily SGAs dose converted to chlorpromazine equivalents (CPZE)

the NBS method, the significant level of FC between pre-treatment and posttreatment FEP patient was set $P < 0.001$ (uncorrected), corresponding to the primary cluster-defining threshold in the NBS approach.

Results

Demographics

Table 1 shows the demographic for FEP and HV groups. There were no significant differences in age ($P = 0.82$), sex ($P = 0.8$) and education ($P = 0.06$) between the FEP-dn and HV groups. The PANSS scores (positive score, $P = 8.44e-07$; negative score, $P = 0.0023$; general score, $P = 1.43e-05$; total score, $P = 5.18e-06$) were significantly decreased in the FEP-2 m group compared to the FEP-dnp group, as revealed by the paired t-test (Table 2 and Figure S1).

Functional activity changes

At baseline, FEP patients showed significantly decreased ReHo values in the right thalamus compared to HV (Fig. 1 A). In contrast to baseline findings, no differences were found in the thalamus after treatment. After two months of follow-up, FEP patients had significantly decreased ReHo values in the lateral and medial occipital cortex (including bilateral cuneus, lingual, fusiform, and superior/middle/inferior occipital cortex (SOG/MOG/IOG)) and increased ReHo values in the bilateral caudate and putamen (Fig. 1B).
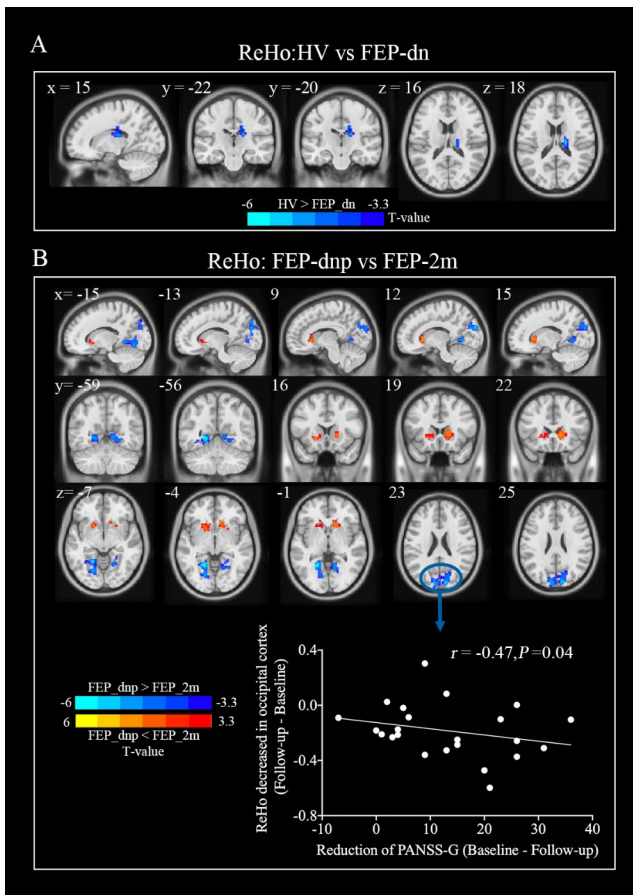
Fig. 1 Group differences of brain functional activity. **(A)** At baseline, patients had decreased ReHo in right thalamus compared with healthy volunteers (two-sample t-test, GRF: voxel $P < 0.001$, cluster $P < 0.05$). Blue voxels: HV > FEP-dn. **(B)** After two-month treatment, patients showed increased ReHo in bilateral caudate and putamen and decreased in the occipital cortex (paired t-test, GRF: voxel $P < 0.001$, cluster $P < 0.05$). Red voxels: FEP-dnp < FEP-2 m; Blue voxels: FEP-dnp > FEP-2 m. The results showed that the longitudinal decrease of ReHo (follow-up minus baseline) in the occipital cortex has a negative correlation with the improvement in general psychotic symptoms (baseline PANSS-G scores minus follow-up PANSS-G scores), indicating the more posttreatment decreases of ReHo in the occipital cortex, the more general symptoms improved ($r = -0.47$, $P = 0.04$). ReHo, regional homogeneity; PANSS-G, PANSS general symptom scores

Abnormal brain FC

At baseline, a subnetwork that included 21 brain regions and 28 edges was identified using the NBS approach ($P < 0.001$, 5000 permutation test, Fig. 2 A), which showed an increase in FC in patients. The primary increase in FC was between the bilateral thalamus and somatomotor network (including bilateral rolandic operculum (ROL), postcentral gyrus (PoCG), superior temporal gyrus (STG), right supplementary motor area (SMA), left paracentral lobule (PCL), heschl gyrus), between right superior frontal gyrus (SFG) and somatomotor network (including left ROL, PCL,
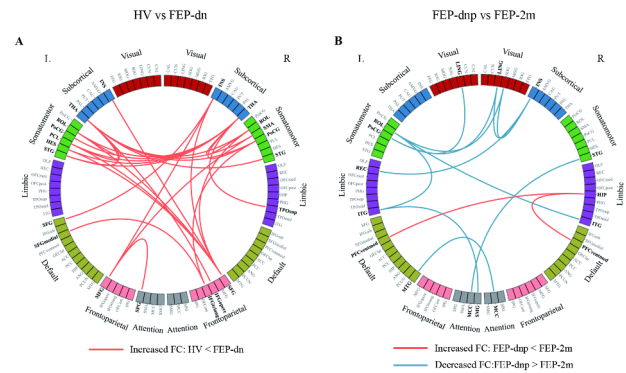

Fig. 2 Baseline and longitudinal altered functional connectivity. **(A)** Significantly altered functional connectivity for the baseline patients. **(B)** Significantly altered functional connectivity for the follow-up patients. The color of the circle denotes the 94 different automatic anatomical labeling 2 (AAL2) regions (abbreviations of AAL2 are listed in Table S5)

heschl gyrus), and between the bilateral insula (INS) and the frontoparietal network (including the right SFG and left middle frontal gyrus (MFG)). After two months of treatment, the patients showed altered functional connectivity, including 17 brain regions and 13 edges ($P < 0.001$, uncorrected, Fig. 2B). The primary decreased FCs were between the visual network (right superior occipital gyrus (SOG) and lingual gyrus (LING)) and right insula, the somatomotor network such as left ROL and PoCG; and between left ROL and bilateral ITG. In addition, patients showed an increase in FC between the right hippocampus and the bilateral ventral medial prefrontal cortex (PFCventmed).

Altered Global Network Topology

Figure 3 and Table S2 showed the group comparison for the global network measures. There were no significant differences in the global network topological parameters at baseline (Fig. 3 A). After two months of treatment, FEP patients showed a decreased clustering coefficient (C_p: $P = 0.03$, $t = -2.30$), characteristic path length (L_p: $P = 0.005$, $t = -3.06$), and normalized characteristic path length (λ: $P = 0.006$, $t = -2.99$), and increased global efficiency (E_g: $P = 0.01$, $t = 2.75$) of the brain network (Fig. 3B). Small worldness was generally evident over a range of graph connection densities. For healthy subjects and FEP patients, their functional networks showed small-world properties in the connection density range of 1– 40% (Fig S2).

Module structure and degree distributions

Figure 4A showed the trend of global modularization in brain networks with a connection density in the range 1–100%. We found that when the modularity was greater
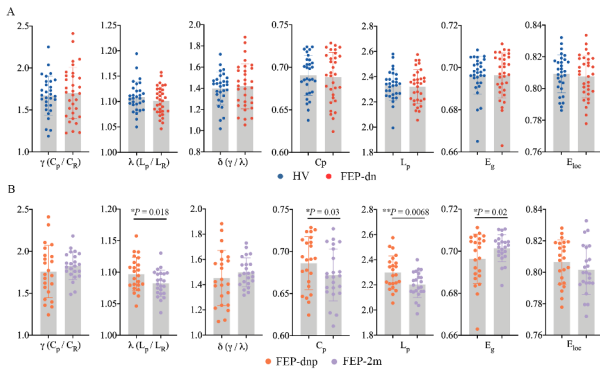
Fig. 3 Group comparison for the global network measures groups. **(A)** At baseline, there were no differences in the AUC of global network measures between patients and healthy volunteers ($P > 0.05$). **(B)** After two-month treatment, patients showed significantly decreased clustering coefficient (C_p) and shortest path length (L_p), and increased efficiency (Eg) (*$P < 0.05$, uncorrected, **$P < 0.05/7 = 0.007$, Bonferroni correction)
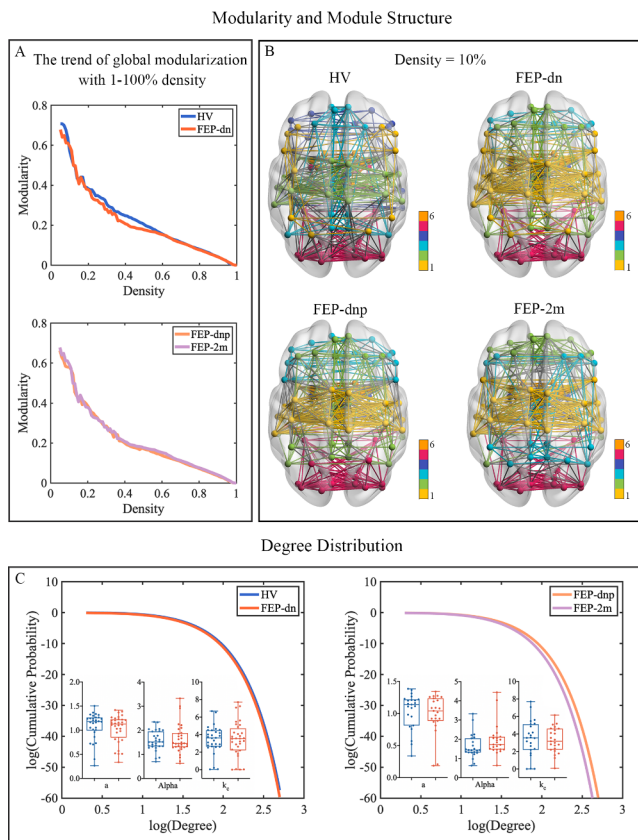

Fig. 4 Module structure and degree distributions (A) The trend of global modularization in brain networks with connection density in the range 1–100%. The modularity of the brain network decreased with the increase of connection density. (B) Visualized brain network diagram with a density of 10%. (C) The cumulative degree distributions were fit in each group. The fitted curves with the median value of the power-law exponent in each group are plotted; (Inset) boxplots represent the within-group distributions and between-group differences in the three parameters: *a, αlpha,* and the exponential cutoff, k_c
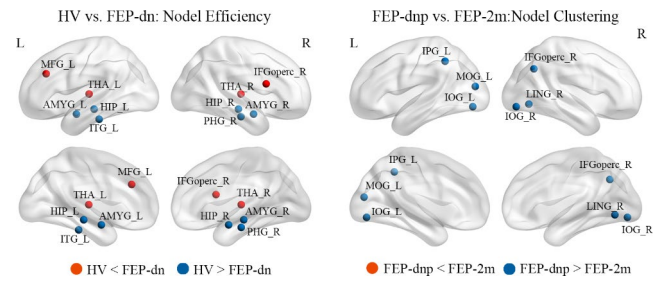
Fig. 5 Group comparison for the nodal topological parameters. **(A)** Regions with significant differences in nodal efficiency between baseline patients and healthy volunteers ($P < 0.05$, FDR-corrected). **(B)** Regions with significant differences in nodal clustering between patients before and after treatment ($P < 0.05$, FDR-corrected)

than 0.3, the density threshold was less than 28%, and all groups had modularity. The modularity of the brain network decreased with increasing connection density. Figure 4B shows a visualized brain network diagram with a density of 10% (minimal value to guarantee full connection of the network). Under the assigned density, the brain network of all groups was divided into six modules, and the different groups have a similar modular partition. The best-fitting form of the degree distribution was generally an exponentially truncated power law. Figure 4C showed that there were no significant differences between HV and FEP-dn and between FEP-dnp and FEP-2 m in terms of mean degree distribution parameters in the small-world regime.

Altered nodal topology characteristics

Compared to HV, patients exhibited significantly increased E_{g_node} in the bilateral thalamus (THA_R/L), left middle frontal gyrus (MFG_L), and the right inferior frontal gyrus of the opercular part (IFGoperc_R), and decreased E_{g_node} in the bilateral amygdala (AMYG_R/L), bilateral hippocampus (HIP_R), right parahippocampal gyrus and left inferior temporal gyrus (ITG_L) compared to HV ($P < 0.05$, FDR-corrected) (Fig. 5A, Table S3). After two months of treatment, patients showed decreased C_{p_node} in bilateral inferior occipital gyrus (IOG_R/L), left middle occipital gyrus (MOG_L), right lingual gyrus (LING_R), and right angular (ANG_R) ($P < 0.05$, FDR-corrected) (Fig. 5B, Table S4). In the correlation analysis, abnormal nodal properties in FEP at baseline and after treatment did not have a significant relationship with PANSS scores.

Relationships between fMRI measures and FEP-related clinical variables

No correlations between ReHo/network parameters (both at the global and regional level) and PANSS scores were found in the drug-naïve FEP patients. In the follow-up analysis,

the results showed that the longitudinal decrease of ReHo (follow-up minus baseline) in the occipital cortex has a negative correlation with the improvement in general psychotic symptoms (baseline PANSS-G scores minus follow-up PANSS-G scores), indicating that the more post-treatment decreases of ReHo in the occipital cortex, the more general symptoms improved ($r = -0.47$, $P = 0.04$) (Fig. 1B).

Discussion

The current study applies ReHo and network connectivity approaches conjunctively to examine complex brain functions in the resting state in FEP patients. Images were collected in the longitudinal study design before and after two months of controlled treatment. Compared to HV, the changes in drug-naïve patients primarily involved the thalamus and its connectivity, including decreased ReHo and increased nodal efficiency in the right thalamus, and increased thalamic-sensorimotor-frontoparietal connectivity. With the improvement of psychosis, patients after treatment showed a wide decrease in neural activity and nodal characteristics in the visual cortex, a decrease in visual-related connections, and increased brain activity in areas related to dopamine. The inherent abnormalities in the FEP patients at baseline differed from the regions affected by the antipsychotic medication.

In the cross-sectional analysis, ReHo and network connectivity abnormalities were predominantly found in the thalamus in drug-naïve FEP patients, which were partly consistent with the previous studies of ReHo and functional connectivity in schizophrenia (Li et al., 2017; Zhao et al., 2019). Recently, increasing neuroimaging studies have explored the role of the thalamus in schizophrenia and have emphasized that disruption of local synchronization of spontaneous activity (i.e., thalamus) may be involved in the psychopathology of schizophrenia (Chen et al., 2013; Liu et al., 2016; Sim et al., 2006). Additionally, previous structural studies also reported reduced thalamic volume and shape changes in the early and chronic stages of schizophrenia (Coscia et al., 2009; Csernansky et al., 2004; Hazlett et al., 1999). These changes in thalamic morphology could contribute to our findings of decreased ReHo in the thalamus. Note that diseases caused by thalamic injury could induce schizophrenia-like syndromes, adding evidence to its core involvement in psychosis (Morel, 2007; Schmahmann, 2003).

The thalamus plays a critical role in coordinating information as it connects to all areas of the cortical system and transmits information to the neocortex (Anticevic et al., 2015). The neural activity alterations of the thalamus, a major 'relay station' of the brain for information exchange,

could alter the flow of information to and within the brain. Indeed, we observed increased connectivity between the thalamus and the motor and somatosensory cortex in drug-naïve FEP patients, which aligns with observations in patients with psychotic disorders, individuals at high risk, and those in early and chronic stages of schizophrenia (Anticevic, 2017; Cho et al., 2019; Dandash et al., 2017). Our results also showed increased nodal efficiency in the right thalamus, confirming the abnormal higher information dissemination ability in this region from the perspective of a network-level (Achard & Bullmore, 2007). The pattern of over-connectivity between the thalamus and sensorimotor cortices has been replicated and identified in the chronic stage of schizophrenia (Cheng et al., 2015; Li et al., 2017). It has been reported that motor and somatosensory connectivity is maximal in adolescence compared with childhood and adulthood, which follows an inverted U-curve (Siris, 1988). Increased thalamic-somatomotor connectivity may result from disruption of refinement for abnormal brain maturation during the transition from adolescence to adulthood in schizophrenia (Woodward et al., 2012). Taken together, we speculate that the thalamus was a core region for the pathogenesis of schizophrenia, and the thalamic functional alterations occurred in the early stage of schizophrenia and persisted as the disease progressed into the chronic phase.

We identified small-world property, network degree distributions, and the module structure of brain network topology in all groups, which is suggestive of a highly conserved general principle of connectome organization. Despite these consistent properties of the functional network of the human brain, we found that patients after treatment showed decreased clustering coefficients and increased global efficiency, which is consistent with a previous study (Hadley et al., 2016). In addition to the abnormal topological properties of the global network, we also found the patients after treatment exhibited lower spontaneous activity and the nodal clustering in the visual-related regions, including LING, MOG, and IOG. The occipital lobe is the main center of visual processing (Rehman & Al Khalili, 2022). Previous studies reported that chronic schizophrenia showed reduced volume and abnormal neural activity in the occipital lobe (Hassaan et al., 2015; Plomp et al., 2013). Given that chronic patients often have exposure to antipsychotic medications, combined with our findings, functional alterations in the visual network may be sensitive to antipsychotic medications. Notably, although significant changes in the occipital cortex in patients after treatment did not have a clear correlation with the dosage of the medication, our results show that the alterations in neural activity in the occipital lobe were found to be correlated with the improvement of cognitive symptoms. In contrast to first-generation antipsychotics, research indicates that SAGs have an early impact on

cognitive symptoms (Riedel et al., 2007). Cognitive symptom deficits have gained much attention in recent years for they are important contributors to the patients' inability to regain function and vocation (Fumagalli et al., 2009; Green et al., 2000). Thus, the improvement of cognitive symptoms may contribute to a better recovery to understand and interact with the social world around. Furthermore, decreased visual-somatomotor-temporal connections were also found in the patients after treatment. As the visual system is at the fore-end of information processing, alterations in neural activation patterns in regions related to visual perception could contribute to the interactions between sensory, auditory, and perceptual functions (Schechter et al., 2005; Silverstein & Keane, 2011). Therefore, our findings of decreased FC in the visual-sensorimotor-temporal gyrus suggest that the medication may help improve psychosis symptoms by modulating sensory networks, such as visual, auditory, and sensorimotor.

Notably, increased brain activity in the striatal regions was reported in the drug-naïve FEP (Hu et al., 2016; Lui et al., 2010), which was not revealed in our dataset. This discrepancy may be due to various diagnoses, imaging protocols, analysis methods, and statistical criteria. The current study used the two-tailed Gaussian random field correction at a stricter level (voxel-wise $P < 0.001$ and cluster-wise $P < 0.05$), and only the most significant changes in the whole brain are identified. These regions would be revealed while using similar/consistent statistical criteria with previous literature (Figure S4). However, increased ReHo was found in the caudate and putamen of FEP after antipsychotic medication. Previous research has highlighted functional alterations in the striatum in patients with schizophrenia after treatment (Kraguljac et al., 2021; Sarpal et al., 2015, 2017). Several neuroimaging studies have also shown that brain activity is elevated in the caudate and putamen of patients with FEP after treatment, although these studies vary in sample size, medication effects, and dosage follow-up interval (Hu et al., 2016; Lahti et al., 2003; Lui et al., 2010). The dopamine hypothesis of schizophrenia is that excessive release of presynaptic dopamine in the striatum is the basis of psychosis (Howes & Kapur, 2009). Antipsychotic treatment can relieve psychosis symptoms by blocking postsynaptic D2 dopamine receptors in the striatum, leading to compensatorily elevated firing activity of dopamine neurons in the striatal regions, including putamen, caudate, and palladium (Howes & Kapur, 2009). Consistent with our findings, Hu et al., also did not find abnormal ReHo values in striatal in FEP at baseline; after treatment, the patient had increased ReHo values in caudate and putamen (Hu et al., 2016). Further studies are warranted to confirm whether there is hyperactivity in the striatum in drug-naïve FEP patients with a large data set with strict statistical power.

By utilizing localized and network analyses, functional dysconnectivity patterns were found to be distinct between the baseline and follow-up analysis of FEP from the local to global aspects. To further verify our results, we also compared the differences between HV and FEP-2 m (Figure S3). Patients after two months of treatment showed a significantly decreased ReHo in the right thalamus and an increase in nodal efficiency in the prefrontal cortex (PFC) compared to HV, which is highly similar to the findings between HV and FEP at baseline, indicating that functional abnormalities in the thalamus and PFC in FEP are a disease-specific pattern and the medication has a limited effect on it. Furthermore, we found a significantly reduced ReHo and nodal clustering in the occipital cortex in patients after treatment compared to HV, which is consistent with our longitudinal analysis, suggesting that these functional changes may be induced by medication. It is common for schizophrenia to relapse after remission of symptoms (Robinson et al., 1999; Thompson et al., 2018). The possible explanation is that antipsychotic medication alleviates psychosis symptoms by affecting the visual-related cortex and dopamine-related areas, but the treatment does not completely modulate the pathophysiology abnormalities in schizophrenia (i.e., the aberrant spontaneous activity and functional connectivities in the thalamus).

There were several limitations in this study. First, only small samples of the follow-up data were included, which limited the power to interpret functional alterations and clinical evaluations. Second, all patients were treated with the SGAs medication. It would be important to determine whether the changes we observed were a general or specific phenomenon across different types of antipsychotics, as the different antipsychotic agents may vary in their potency and effects on brain function (Tarcijonas & Sarpal, 2019). Third, although fMRI measurements appear to have a moderate test-retest reliability (Li et al., 2012), the lack of repeated fMRI scans for the HV group is a limitation, as we cannot entirely rule out the post-treatment possibility that functional changes could be a time-dependent change during the test-retest period. Finally, fMRI measures a surrogate signal that does not represent the actual neural activity like all hemodynamic-based modalities (Logothetis, 2008). Although functional correlations between time series are widely used to represent the edges of fMRI networks, the underlying biological substrate of this functional connectivity is not well characterized.

Conclusions

With the rs-fMRI datasets and the systematic evaluation of patients before and after antipsychotic treatment, our results show that functional abnormalities in the thalamus are the key regions involved in the pathophysiology of schizophrenia. After two months of antipsychotic treatment, changes in fMRI measurement in FEP patients were mainly distributed in the striatum and visual-related occipital cortex. Although antipsychotic medication alleviates psychotic symptoms after onset, only a few characteristics of medicated-effect regions were found to be associated with symptoms improvement. Combining regional neural activity and network connectivity analysis provides a systemic understanding of schizophrenia pathogenesis and the underlying neural mechanisms of antipsychotic treatment effects.

Declarations

References

Achard, S., & Bullmore, E. (2007). Efficiency and cost of economical brain functional networks. *Plos Computational Biology*, *3*(2), e17. https://doi.org/10.1371/journal.pcbi.0030017

Achard, S., Salvador, R., Whitcher, B., Suckling, J., & Bullmore, E. (2006). A resilient, low-frequency, small-world human brain functional network with highly connected association cortical hubs. *Journal Of Neuroscience*, *26*(1), 63–72. https://doi.org/10.1523/jneurosci.3874-05.2006

Anticevic, A. (2017). Understanding the role of thalamic circuits in schizophrenia neuropathology. *Schizophrenia Research*, *180*, 1–3. https://doi.org/10.1016/j.schres.2016.11.044

Anticevic, A., Haut, K., Murray, J. D., Repovs, G., Yang, G. J., Diehl, C., & Cannon, T. D. (2015). Association of Thalamic Dysconnectivity and Conversion to Psychosis in Youth and Young Adults at Elevated Clinical Risk. *JAMA Psychiatry*, *72*(9), 882–891. https://doi.org/10.1001/jamapsychiatry.2015.0566

Association, A. P. (1994). *Diagnostic and Statistical Manual of Mental Disorders (DSM-IV-TR)*

Bullmore, E., & Sporns, O. (2009). Complex brain networks: graph theoretical analysis of structural and functional systems. *Nature Reviews Neuroscience*, *10*(3), 186–198. https://doi.org/10.1038/nrn2575

Chen, J., Xu, Y., Zhang, K., Liu, Z., Xu, C., Shen, Y., & Xu, Q. (2013). Comparative study of regional homogeneity in schizophrenia and major depressive disorder. *Am J Med Genet B Neuropsychiatr Genet*, *162b*(1), 36–43. https://doi.org/10.1002/ajmg.b.32116

Cheng, W., Palaniyappan, L., Li, M., Kendrick, K. M., Zhang, J., Luo, Q., & Feng, J. (2015). Voxel-based, brain-wide association study of aberrant functional connectivity in schizophrenia implicates thalamocortical circuitry. *NPJ Schizophr*, *1*, 15016. https://doi.org/10.1038/npjschz.2015.16

Cho, K. I. K., Kim, M., Yoon, Y. B., Lee, J., Lee, T. Y., & Kwon, J. S. (2019). Disturbed thalamocortical connectivity in unaffected relatives of schizophrenia patients with a high genetic loading. *Australian And New Zealand Journal Of Psychiatry*, *53*(9), 889–895. https://doi.org/10.1177/0004867418824020

Clauset, A., Newman, M. E., & Moore, C. (2004). Finding community structure in very large networks. *Phys Rev E Stat Nonlin Soft Matter Phys*, *70*(6 Pt 2), 066111. https://doi.org/10.1103/PhysRevE.70.066111

Coscia, D. M., Narr, K. L., Robinson, D. G., Hamilton, L. S., Sevy, S., Burdick, K. E., & Szeszko, P. R. (2009). Volumetric and shape analysis of the thalamus in first-episode schizophrenia. *Human Brain Mapping*, *30*(4), 1236–1245. https://doi.org/10.1002/hbm.20595

Crossley, N. A., Marques, T. R., Taylor, H., Chaddock, C., Dell'Acqua, F., Reinders, A. A., & Dazzan, P. (2017). Connectomic correlates of response to treatment in first-episode psychosis. *Brain*, *140*(2), 487–496. https://doi.org/10.1093/brain/aww297

Csernansky, J. G., Schindler, M. K., Splinter, N. R., Wang, L., Gado, M., Selemon, L. D., & Miller, M. I. (2004). Abnormalities of thalamic volume and shape in schizophrenia. *American Journal Of Psychiatry*, *161*(5), 896–902. https://doi.org/10.1176/appi.ajp.161.5.896

Dandash, O., Pantelis, C., & Fornito, A. (2017). Dopamine, fronto-striato-thalamic circuits and risk for psychosis.

Schizophrenia Research, *180*, 48–57. https://doi.org/10.1016/j.schres.2016.08.020

Del Fabro, L., Schmidt, A., Fortea, L., Delvecchio, G., D'Agostino, A., Radua, J., & Brambilla, P. (2021). Functional brain network dysfunctions in subjects at high-risk for psychosis: A meta-analysis of resting-state functional connectivity. *Neuroscience And Biobehavioral Reviews*, *128*, 90–101. https://doi.org/10.1016/j.neubiorev.2021.06.020

Dixon, L., Postrado, L., Delahanty, J., Fischer, P. J., & Lehman, A. (1999). The association of medical comorbidity in schizophrenia with poor physical and mental health. *The Journal Of Nervous And Mental Disease*, *187*(8), 496–502. https://doi.org/10.1097/00005053-199908000-00006

Elhamaoui, S., Yaalaoui, S., Moussaoui, D., & Battas, O. (2003). Two years follow-up of patients with acute psychotic access: evolutionary modes and prognosis. *L Encéphale*, *29*(5), 425–429

Fumagalli, F., Frasca, A., Racagni, G., & Riva, M. A. (2009). Cognitive effects of second-generation antipsychotics: current insights into neurochemical mechanisms. *Cns Drugs*, *23*(7), 603–614. https://doi.org/10.2165/00023210-200923070-00005

Ganella, E. P., Seguin, C., Pantelis, C., Whittle, S., Baune, B. T., Olver, J., & Bartholomeusz, C. F. (2018). Resting-state functional brain networks in first-episode psychosis: A 12-month follow-up study. *Australian And New Zealand Journal Of Psychiatry*, *52*(9), 864–875. https://doi.org/10.1177/0004867418775833

Girvan, M., & Newman, M. E. (2002). Community structure in social and biological networks. *Proc Natl Acad Sci U S A*, *99*(12), 7821–7826. https://doi.org/10.1073/pnas.122653799

Green, M. F., Kern, R. S., Braff, D. L., & Mintz, J. (2000). Neurocognitive deficits and functional outcome in schizophrenia: are we measuring the "right stuff"? *Schizophrenia Bulletin*, *26*(1), 119–136. https://doi.org/10.1093/oxfordjournals.schbul.a033430

Greve, D. N., & Fischl, B. (2009). Accurate and robust brain image alignment using boundary-based registration. *Neuroimage*, *48*(1), 63–72. https://doi.org/10.1016/j.neuroimage.2009.06.060

Guo, W., Liu, F., Chen, J., Wu, R., Li, L., Zhang, Z., & Zhao, J. (2018). Treatment effects of olanzapine on homotopic connectivity in drug-free schizophrenia at rest. *The World Journal Of Biological Psychiatry : The Official Journal Of The World Federation Of Societies Of Biological Psychiatry*, *19*(sup3), S106–s114. https://doi.org/10.1080/15622975.2017.1346280

Hadley, J. A., Kraguljac, N. V., White, D. M., Hoef, V., Tabora, L., J., & Lahti, A. C. (2016). Change in brain network topology as a function of treatment response in schizophrenia: a longitudinal resting-state fMRI study using graph theory. *NPJ Schizophr*, *2*, 16014. https://doi.org/10.1038/npjschz.2016.14

Hassaan, T., Muhammad, F., & Uzma, F. (2015). Alterations of the occipital lobe in schizophrenia. *Neurosciences*, *20*(3), 213–224. https://doi.org/10.17712/nsj.2015.3.20140757

Hazlett, E. A., Buchsbaum, M. S., Byne, W., Wei, T. C., Spiegel-Cohen, J., Geneve, C., & Siever, L. J. (1999). Three-dimensional analysis with MRI and PET of the size, shape, and function of the thalamus in the schizophrenia spectrum. *American Journal Of Psychiatry*, *156*(8), 1190–1199. https://doi.org/10.1176/ajp.156.8.1190

He, Z., Deng, W., Li, M., Chen, Z., Jiang, L., Wang, Q., & Li, T. (2013). Aberrant intrinsic brain activity and cognitive deficit in first-episode treatment-naive patients with schizophrenia. *Psychological Medicine*, *43*(4), 769–780. https://doi.org/10.1017/s0033291712001638

Howes, O. D., & Kapur, S. (2009). The dopamine hypothesis of schizophrenia: version III–the final common pathway. *Schizophrenia Bulletin*, *35*(3), 549–562. https://doi.org/10.1093/schbul/sbp006

Hu, M. L., Zong, X. F., Zheng, J. J., Pantazatos, S. P., Miller, J. M., Li, Z. C., & Sang, D. E. (2016). Short-term Effects of Risperidone Monotherapy on Spontaneous Brain Activity in First-episode Treatment-naïve Schizophrenia Patients: A Longitudinal fMRI Study. *Scientific Reports*, *6*, 34287. https://doi.org/10.1038/srep34287

Huang, X. Q., Lui, S., Deng, W., Chan, R. C. K., Wu, Q. Z., Jiang, L. J., & Li, X. L. (2010). Localization of cerebral functional deficits in treatment-naive, first-episode schizophrenia using resting-state fMRI. *Neuroimage*, *49*(4), 2901–2906. https://doi.org/10.1016/j.neuroimage.2009.11.072

Kay, S. R., Fiszbein, A., & Opler, L. A. (1987). The positive and negative syndrome scale (PANSS) for schizophrenia. *Schizophrenia Bulletin*, *13*(2), 261–276. https://doi.org/10.1093/schbul/13.2.261

Kraguljac, N. V., McDonald, W. M., Widge, A. S., Rodriguez, C. I., Tohen, M., & Nemeroff, C. B. (2021). Neuroimaging Biomarkers in Schizophrenia. *American Journal Of Psychiatry*, *178*(6), 509–521. https://doi.org/10.1176/appi.ajp.2020.20030340

Kraguljac, N. V., White, D. M., Hadley, J. A., Visscher, K., Knight, D., ver, Hoef, L., & Lahti, A. C. (2016). Abnormalities in large scale functional networks in unmedicated patients with schizophrenia and effects of risperidone. *Neuroimage Clin*, *10*, 146–158. https://doi.org/10.1016/j.nicl.2015.11.015

Lahti, A. C., Holcomb, H. H., Weiler, M. A., Medoff, D. R., & Tamminga, C. A. (2003). Functional effects of antipsychotic drugs: comparing clozapine with haloperidol. *Biological Psychiatry*, *53*(7), 601–608. https://doi.org/10.1016/s0006-3223(02)01602-5

Li, F., Lui, S., Yao, L., Hu, J., Lv, P., Huang, X., & Gong, Q. (2016a). Longitudinal Changes in Resting-State Cerebral Activity in Patients with First-Episode Schizophrenia: A 1-Year Follow-up Functional MR Imaging Study. *Radiology*, *279*(3), 867–875. https://doi.org/10.1148/radiol.2015151334

Li, F., Lui, S., Yao, L., Hu, J., Lv, P., Huang, X., & Gong, Q. J. R. (2016b). Longitudinal Changes in Resting-State Cerebral Activity in Patients with First-Episode Schizophrenia: A 1-Year Follow-up Functional MR Imaging Study. *279*(3),151334. https://doi.org/10.1148/radiol.2015151334

Li, T., Wang, Q., Zhang, J., Rolls, E. T., Yang, W., Palaniyappan, L., & Feng, J. (2017). Brain-Wide Analysis of Functional Connectivity in First-Episode and Chronic Stages of Schizophrenia. *Schizophrenia Bulletin*, *43*(2), 436–448. https://doi.org/10.1093/schbul/sbw099

Li, Z., Kadivar, A., Pluta, J., Dunlop, J., & Wang, Z. (2012). Test-retest stability analysis of resting brain activity revealed by blood oxygen level-dependent functional MRI. *Journal Of Magnetic Resonance Imaging*, *36*(2), 344–354. https://doi.org/10.1002/jmri.23670

Liu, C., Xue, Z., Palaniyappan, L., Zhou, L., Liu, H., Qi, C., & Pu, W. (2016). Abnormally increased and incoherent resting-state activity is shared between patients with schizophrenia and their unaffected siblings. *Schizophrenia Research*, *171*(1–3), 158–165. https://doi.org/10.1016/j.schres.2016.01.022

Lo, C. Y., Su, T. W., Huang, C. C., Hung, C. C., Chen, W. L., Lan, T. H., & Bullmore, E. T. (2015). Randomization and resilience of brain functional networks as systems-level endophenotypes of schizophrenia. *Proc Natl Acad Sci U S A*, *112*(29), 9123–9128. https://doi.org/10.1073/pnas.1502052112

Logothetis, N. K. (2008). What we can do and what we cannot do with fMRI. *Nature*, *453*(7197), 869–878. https://doi.org/10.1038/nature06976

Lui, S., Li, T., Deng, W., Jiang, L., Wu, Q., Tang, H., & Gong, Q. (2010). Short-term effects of antipsychotic treatment on cerebral function in drug-naive first-episode schizophrenia revealed by "resting state" functional magnetic resonance imaging. *Archives Of General Psychiatry*, *67*(8), 783–792. https://doi.org/10.1001/archgenpsychiatry.2010.84

McGrath, J., Saha, S., Chant, D., & Welham, J. (2008). Schizophrenia: a concise overview of incidence, prevalence, and mortality.

Epidemiologic Reviews, *30*, 67–76. https://doi.org/10.1093/epirev/mxn001

Morel, A. (2007). The thalamus and behavior: effects of anatomically distinct strokes. *Neurology*, *68*(19), 1640; author reply 1640–1641. https://doi.org/10.1212/01.wnl.0000265608.00944.ff

Nina, V., Kraguljac, D., White, M., & Ann (2016). Aberrant Hippocampal Connectivity in Unmedicated Patients With Schizophrenia and Effects of Antipsychotic Medication: A Longitudinal Resting State Functional MRI Study.Schizophrenia Bulletin, *42*(4)

Patel, A. X., Kundu, P., Rubinov, M., Jones, P. S., Vértes, P. E., Ersche, K. D., & Bullmore, E. T. (2014). A wavelet method for modeling and despiking motion artifacts from resting-state fMRI time series. *Neuroimage*, *95*(100), 287–304. https://doi.org/10.1016/j.neuroimage.2014.03.012

Plomp, G., Roinishvili, M., Chkonia, E., Kapanadze, G., Kereselidze, M., Brand, A., & Herzog, M. H. (2013). Electrophysiological evidence for ventral stream deficits in schizophrenia patients. *Schizophrenia Bulletin*, *39*(3), 547–554. https://doi.org/10.1093/schbul/sbr175

Rehman, A., & Al Khalili, Y. (2022). Neuroanatomy, Occipital Lobe. In *StatPearls*. StatPearls Publishing Copyright (2022). © StatPearls Publishing LLC

Riedel, M., Müller, N., Spellmann, I., Engel, R. R., Musil, R., Valdevit, R., & Möller, H. J. (2007). Efficacy of olanzapine versus quetiapine on cognitive dysfunctions in patients with an acute episode of schizophrenia. *Eur Arch Psychiatry Clin Neurosci*, *257*(7), 402–412. https://doi.org/10.1007/s00406-007-0748-9

Robinson, D., Woerner, M. G., Alvir, J. M., Bilder, R., Goldman, R., Geisler, S., & Lieberman, J. A. (1999). Predictors of relapse following response from a first episode of schizophrenia or schizoaffective disorder. *Archives Of General Psychiatry*, *56*(3), 241–247. https://doi.org/10.1001/archpsyc.56.3.241

Rolls, E. T., Joliot, M., & Tzourio-Mazoyer, N. (2015). Implementation of a new parcellation of the orbitofrontal cortex in the automated anatomical labeling atlas. *Neuroimage*, *122*, 1–5. https://doi.org/10.1016/j.neuroimage.2015.07.075

Sarpal, D. K., Robinson, D. G., Fales, C., Lencz, T., Argyelan, M., Karlsgodt, K. H., & Malhotra, A. K. (2017). Relationship between Duration of Untreated Psychosis and Intrinsic Corticostriatal Connectivity in Patients with Early Phase Schizophrenia. *Neuropsychopharmacology : Official Publication Of The American College Of Neuropsychopharmacology*, *42*(11), 2214–2221. https://doi.org/10.1038/npp.2017.55

Sarpal, D. K., Robinson, D. G., Lencz, T., Argyelan, M., Ikuta, T., Karlsgodt, K., & Malhotra, A. K. (2015). Antipsychotic treatment and functional connectivity of the striatum in first-episode schizophrenia. *JAMA Psychiatry*, *72*(1), 5–13. https://doi.org/10.1001/jamapsychiatry.2014.1734

Schechter, I., Butler, P. D., Zemon, V. M., Revheim, N., Saperstein, A. M., Jalbrzikowski, M., & Javitt, D. C. (2005). Impairments in generation of early-stage transient visual evoked potentials to magno- and parvocellular-selective stimuli in schizophrenia. *Clinical Neurophysiology*, *116*(9), 2204–2215. https://doi.org/10.1016/j.clinph.2005.06.013

Schmahmann, J. D. (2003). Vascular syndromes of the thalamus. *Stroke*, *34*(9), 2264–2278. https://doi.org/10.1161/01.Str.0000087786.38997.9e

Silverstein, S. M., & Keane, B. P. (2011). Vision science and schizophrenia research: toward a re-view of the disorder. Editors' introduction to special section. *Schizophrenia Bulletin*, *37*(4), 681–689. https://doi.org/10.1093/schbul/sbr053

Sim, K., Cullen, T., Ongur, D., & Heckers, S. (2006). Testing models of thalamic dysfunction in schizophrenia using neuroimaging. *J Neural Transm (Vienna)*, *113*(7), 907–928. https://doi.org/10.1007/s00702-005-0363-8

Siris, S. G. (1988). Implications of normal brain development for the pathogenesis of schizophrenia. *Archives Of General Psychiatry*, *45*(11), 1055. https://doi.org/10.1001/archpsyc.1988.01800350089019

Tarcijonas, G., & Sarpal, D. K. (2019). Neuroimaging markers of antipsychotic treatment response in schizophrenia: An overview of magnetic resonance imaging studies. *Neurobiology Of Diseases*, *131*, 104209. https://doi.org/10.1016/j.nbd.2018.06.021

Thompson, A., Winsper, C., Marwaha, S., Haynes, J., Alvarez-Jimenez, M., Hetrick, S., & Sullivan, S. A. (2018). Maintenance antipsychotic treatment versus discontinuation strategies following remission from first episode psychosis: systematic review. *BJPsych Open*, *4*(4), 215–225. https://doi.org/10.1192/bjo.2018.17

van den Heuvel, M. P., Sporns, O., Collin, G., Scheewe, T., Mandl, R. C., Cahn, W., & Kahn, R. S. (2013). Abnormal rich club organization and functional brain dynamics in schizophrenia. *JAMA Psychiatry*, *70*(8), 783–792. https://doi.org/10.1001/jamapsychiatry.2013.1328

Wang, J., Wang, X., Xia, M., Liao, X., Evans, A., & He, Y. (2015). GRETNA: a graph theoretical network analysis toolbox for imaging connectomics. *Frontiers In Human Neuroscience*, *9*, 386. https://doi.org/10.3389/fnhum.2015.00386

Wang, L. X., Guo, F., Zhu, Y. Q., Wang, H. N., Liu, W. M., Li, C., & Yin, H. (2019). Effect of second-generation antipsychotics on brain network topology in first-episode schizophrenia: A longitudinal rs-fMRI study. *Schizophrenia Research*, *208*, 160–166. https://doi.org/10.1016/j.schres.2019.03.015

Wang, Y., Tang, W., Fan, X., Zhang, J., Geng, D., Jiang, K., & Liu, D. (2017). Resting-state functional connectivity changes within the default mode network and the salience network after antipsychotic treatment in early-phase schizophrenia. *Neuropsychiatric Disease And Treatment*, *13*, 397–406. https://doi.org/10.2147/ndt.S123598

Watts, D. J., & Strogatz, S. H. (1998). Collective dynamics of 'small-world' networks.Nature

Woodward, N. D., Karbasforoushan, H., & Heckers, S. (2012). Thalamocortical dysconnectivity in schizophrenia. *American Journal Of Psychiatry*, *169*(10), 1092–1099. https://doi.org/10.1176/appi.ajp.2012.12010056

Yeo, B. T., Krienen, F. M., Sepulcre, J., Sabuncu, M. R., Lashkari, D., Hollinshead, M., & Buckner, R. L. (2011). The organization of the human cerebral cortex estimated by intrinsic functional connectivity. *Journal Of Neurophysiology*, *106*(3), 1125–1165. https://doi.org/10.1152/jn.00338.2011

Zang, Y., Jiang, T., Lu, Y., He, Y., & Tian, L. (2004). Regional homogeneity approach to fMRI data analysis. *Neuroimage*, *22*(1), 394–400. https://doi.org/10.1016/j.neuroimage.2003.12.030

Zhao, X., Yao, J., Lv, Y., Zhang, X., Han, C., Chen, L., & Sui, Y. (2019). Abnormalities of regional homogeneity and its correlation with clinical symptoms in Naïve patients with first-episode schizophrenia. *Brain Imaging Behav*, *13*(2), 503–513. https://doi.org/10.1007/s11682-018-9882-4